EXPERIMENTAL DEFORMATION OF SERPENTINITE AND ITS TECTONIC IMPLICATIONS

C. B. RALEIGH
AND
M. S. PATERSON

A Reprint from

AUGUST 15, 1965

Journal of Geophysical Research

VOLUME 70 NUMBER 16

PUBLISHED BY
THE AMERICAN GEOPHYSICAL UNION

JOURNAL OF GEOPHYSICAL RESEARCH VOL. 70, NO. 16 AUGUST 15, 1965

Experimental Deformation of Serpentinite and Its Tectonic Implications

C. B. RALEIGH AND M. S. PATERSON

Department of Geophysics and Geochemistry
Australian National University, Canberra

Abstract. Experimental investigation into the strength and ductility of serpentinite at temperatures to 700°C and confining pressures to 5 kb has yielded results important to the understanding of the role of serpentinite in orogenesis. Sealed specimens of antigorite-chrysotile serpentinite, with ultimate strength comparable to that of granite at room temperature, showed a marked weakening above 500–600°C; a mesh-textured serpentinite containing lizardite, chrysotile, and a minor amount of brucite showed a similar loss of strength at 300–350°C. Brittleness always accompanied the high-temperature weakening, although the samples showing high strength at lower temperatures were often ductile. Petrographic and X-ray examinations reveal that serpentine in the weakened and embrittled specimens has undergone partial dehydration to forsterite and talc. The embrittlement and weakening is attributed to a reduction in the effective confining pressure due to the pore pressure of the water released during dehydration and to a loss in cohesive strength due to changes in the structure upon dehydration. The hypothesis of tectonic emplacement of serpentinites of the alpine type thus becomes highly plausible at temperatures great enough for dehydration weakening, while being difficult to accept at lower temperatures where the strength of the serpentinite is high. Weakening upon heating to the appropriate dehydration temperature in the range 300–600°C of a partially serpentinized oceanic lower crust or upper mantle should also serve to concentrate deformation in the heated belt, thus facilitating mountain building. The embrittlement associated with dehydration extends the maximum theoretical depth for brittle fracture in the mantle to that of the deepest hydrated phases.

INTRODUCTION

Alpine serpentinites are found in almost every large-scale belt of intensely deformed rocks—notably in alpine mountain chains and island arcs. In other settings they are relatively rare. Serpentinite is thought by some [*Hess,* 1955; *Dietz,* 1962] to constitute the deepest seismic layer in the oceanic crust, and if, as seems likely, peridotite is an important constituent of the upper mantle, small amounts of serpentinite may well be present at shallow depths in the mantle. The mechanical properties of serpentinite are therefore of particular interest in discussions of large-scale orogenic events and of the deformations of the oceanic crust and mantle implied in theories of continental drift or convection.

Knowledge of the strength of serpentinite at elevated pressure and temperatures is especially important in understanding the emplacement of alpine ultramafics. These occur most commonly as fault-bounded slivers in sedimentary and volcanic country rock, and it has been suggested [*Bowen and Tuttle,* 1949; *de Roever,* 1957] that they have been sheared from deep intrusions or from the upper mantle by large reverse faults and forcibly emplaced in the overlying crustal rocks. At great depths, where the temperature is high, the vertical movements were thought by Bowen and Tuttle to occur by plastic flow within the olivine crystals; at higher levels, where the peridotite has cooled below 500°C, serpentinization may proceed in the presence of water, and further movement is presumed to be facilitated by the weaker, plastic shell of serpentinite. A somewhat similar view was advanced by *Hess* [1955], who envisioned the large vertical movements to be the sum of small shear displacements in numerous faults in the serpentinite skin on the peridotite and likened the process of intrusion to squeezing a watermelon seed between two fingers.

Contrary to these notions of serpentinite as an especially weak rock, *Paterson* [1964] found that in short-time tests at room temperature and 8 kb confining pressure it has approximately the strength of granite. *Handin* [1964]

tested specimens of serpentinite from the Amsoc drill hole on Puerto Rico and found a strength as high as that of most other rocks at room temperature and 1 kb confining pressure. However, he found the strength to decrease steadily to less than half the room temperature value in experiments up to 200°C. This large decrease was attributed to the weakening effect of internal pressure of water. D. T. Griggs (personal communication, 1962) found a large decrease in the strength of serpentinite at 300°C from its strength at lower temperatures.

Rubey and Hubbert [1959, p. 185] suggested that metamorphism of hydrated minerals would result in a reduction of strength due to the effect of pore pressure of the water released in lowering the effective confining pressure so that a reduction in strength in serpentinite might also be expected when the temperature is raised to that at which the serpentine dehydrates to olivine and talc. The water released should give rise to a pore pressure which will reduce the 'effective' confining pressure. It has been predicted theoretically [*Hubbert and Rubey,* 1959] and shown experimentally [*Handin et al.,* 1963] that, provided there is adequate permeability within the specimen and no complicating chemical effects, the effect of a pore pressure on the stress for brittle failure of a sealed rock specimen can often be represented, as in the case of soils [*Terzhagi,* 1936], by a modification of the Coulomb–Navier equation so that

$$\tau = \tau_0 + (\sigma - p) \tan \phi \qquad (1)$$

where $\sigma - p$ has replaced σ, the normal stress on the plane of failure; τ is the shear stress on the plane of failure, p is the pore pressure, and τ_0 and tan ϕ are the constants usually known as the 'cohesion' and the 'coefficient of internal friction,' respectively. Thus, when p approaches σ in magnitude, the shear strength approaches τ_0, which, for most rocks, is small relative to their strength at several kilobars of confining pressure in the absence of a pore pressure. *Heard and Rubey* [1963] have confirmed this prediction of strength loss upon dehydration by finding a tenfold reduction in the ultimate strength of gypsum at its dehydration temperature in tests at 5 kb confining pressure.

In the present experiments our objective was to determine the magnitude of any such weakening effect in serpentinite in a range of temperature, pressure, and composition which is thought to provide a first approximation to natural conditions in the crust and shallow oceanic mantle. The effect of varying the strain rate, although very important to geological interpretation, was not included in this study. However, the experiments permit some observations on the effect of pressure and temperature on the brittle-ductile transition in serpentinite.

Experimental Procedure

The stress-strain relations were measured in a new apparatus for investigating mechanical properties of materials at high pressure and temperature. This apparatus is similar in function to the 800°C apparatus described by *Griggs et al.* [1960]. It is based on the same layout as was used in a previous room temperature apparatus [*Paterson,* 1964; cf. *Griggs,* 1936] but has a pressure vessel fitted with an internal furnace. Temperature was monitored by a thermocouple in the furnace wall, periodically calibrated against a thermocouple in the center of a 'dummy' specimen connected to a hollow piston. If allowance is made for some drift between calibrations, temperatures are probably accurate to ±10°C. The temperature variation along the specimen did not exceed about 5°C and was usually less. Temperatures up to 700°C and confining pressures to 5 kb were used in these experiments. The pressure medium was argon.

The specimens were cylinders of 1-cm diameter and 2- or 2.5-cm length, prepared by drilling from blocks of serpentinite with a diamond core drill and grinding the ends parallel within 0.01 mm (no significant difference in results from specimens 2 and 2.5 cm long was observed). The specimens were dried for at least 24 hours at 120°C. For the testing, the specimen was assembled between high-speed tool steel end pieces in an annealed copper jacket of 0.010-inch wall thickness. The jacket was sealed to a high-speed tool steel piston at each end, using a mechanical closure similar in principle to that used by *Handin* [1953] but with a cylindrical rather than a conical sealing area onto which the steel rings were forced with interference fit over the copper. The gas pressure medium was therefore prevented from entering the specimen. Unsuccessful initial sealing of the

jacket could usually be detected after the experiment by submerging the assembly in water and noting escape of bubbles; when leaks were so detected, the specimen behavior was erratic, being generally weaker and more brittle than expected from the other experiments, and the results were rejected. However, after overcoming some early difficulties, relatively few runs have had to be rejected for this reason.

In the tests, the confining pressure was first raised and then the jacketed specimen was heated for a time which varied from 30 minutes to 7 hours. At the end of this period and at the same temperature, axial load was applied and the specimen strained at a rate of 7×10^{-4} sec^{-1}, usually up to strains of 5 to 10% but less if a load drop occurred, especially at the highest temperatures. The furnace power was cut off after the load was released and the temperature dropped to below 100°C within 5 to 10 minutes before the confining pressure was reduced.

In deriving the stress-strain curves, we have corrected the load for piston friction, determined before contact with the specimen and usually about 500 kg, and have calculated the stress on the basis of the original cross-sectional area.

The spread in ultimate strengths of any one rock type at a given pressure and temperature is no more than 20%. The accuracy of stress measurement is estimated to be ±0.2 kb.

Specimen Materials

Four rocks were used in the experiments: two antigorite-chrysotile serpentinites from Cabramurra and Tumut Pond, New South Wales, and two mesh-texture serpentinites from Fidalgo Island, Skagit County, Washington, one of which contains about 60% of olivine and enstatite.

The antigorite serpentinites consist of approximately rectangular flakes of serpentine in a flare texture, that is, in radiating aggregates. The grains show little undulatory extinction and no kink bands, which suggests that the rocks have suffered little or no postcrystalline plastic strain. The Cabramurra serpentinite contains antigorite and clino-chrysotile[1] giving

Antigorite, angstroms	Clino-chrysotile, angstroms	Lizardite, angstroms
7.30	7.36	7.36
2.52	4.58	4.62
	2.66	2.15
	2.45	1.794
		1.503

(001) reflections of equal height on the X-ray diffractometer. The quantities of other phases estimated from sections include about 10% of magnetite, 5 to 10% olivine, 2% magnesite, and minor talc and chlorite. The Tumut Pond serpentinite is similar but contains no olivine and less magnetite. Other diffractometer peaks for the antigorite serpentinites correspond to *d*-spacings of 4.44, 2.62, 2.40, and 1.560 A, with heights no greater than 2% of that corresponding to the 7.3 A serpentine spacing; these may indicate the presence of other phases of unknown composition.

The serpentinite and partly serpentinized peridotite from Fidalgo Island contain a mixture of lizardite and clino-chrysotile, with some brucite (2% when determined by the method of *Hess and Otalora* [1964]) and less than 1% chromite. The grains are arranged in the typical mesh network, each mesh having an isotropic core. A very fine dust of opaque material is present throughout and is probably magnetite, since a chemical analysis kindly supplied by John Easton gave FeO = 3.33%, Fe_2O_3 = 3.25%.

Experimental Results

Room Temperature Experiments

Stress-strain results. The gradual transition of Cabramurra serpentinite from brittle behavior at the lower pressures, with sudden loss of strength at failure, to predominantly ductile behavior at 5 kb, with a smoothly rounded stress-strain curve is shown in Figure 1. The shape of the curve is not reproducible in the transitional specimens, but specimens that are clearly ductile or brittle always give curves similar to *D* and *A*, respectively.

At confining pressures of up to 2 kb, failure generally takes place along a single shear fracture before appreciable plastic deformation has occurred and the failure conditions approximately fit a Coulomb–Navier criterion. Thus, for the two antigorite serpentinites, on which

[1] The serpentine minerals were distinguished on the basis of the following combinations of *d*-spacings characteristic of each variety [*Whittaker and Zussman*, 1956].

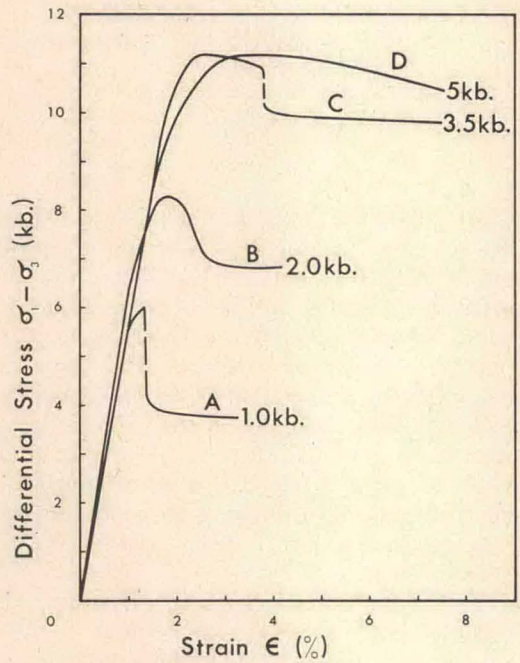

Fig. 1. Stress-strain curves for Cabramurra serpentinite at room temperature.

most of the room temperature measurements were made, the stress difference, $\sigma_1 - \sigma_3$, at brittle failure is a linear function of the minimum principal stress (confining pressure) σ_3:

$$\sigma_1 - \sigma_3 = 3.3 + 2.4\sigma_3 \qquad (2)$$

where σ_1 and σ_3 are in kilobars and compressive stresses are positive. The individual results (Table 1) are plotted in Figure 2. The corresponding Mohr envelope or Coulomb–Navier condition [*Jaeger,* 1962, chapter 2] is the straight line

$$\tau = 0.9 + 0.65\sigma \qquad (3)$$

giving $\tau_0 = 0.9$ kb and $\tan \phi = 0.65$ or $\phi = 33°$. The angle $\theta = \pi/4 - \phi/2$ between the fracture plane and the direction of the maximum principal stress according to the Mohr theory is therefore 29°, which agrees well with the average value of 30° measured on the specimens; however, the measured values spread up to 20% from the average, with a tendency for θ to increase with pressure. Slickensides are present on the shear surfaces and are better developed at 1 kb and above than at the lower confining pressures.

At 3.5 kb confining pressure, some macroscopic evidence of ductility appears; instead of the single shear fracture typical of lower pressures, a system of fine conjugate shears is present in addition to one or two major fault zones of up to ½-mm width in which a combination of plastic deformation and fracturing has occurred. At 5 kb, deformation is distributed through a broad band crossing the specimen diagonally, accompanied by a few minor faults. In a specimen of Cabramurra serpentinite tested at 8 kb the deformation was distributed almost uniformly throughout.

Further straining after the sharp drop in load accompanying brittle failure causes sliding on the fracture surfaces, the resistance to sliding being represented by the flat part of the stress-strain curve after the drop (cf. curves *A* and *B,* Figure 1). The ratio of the shear stress and normal stress components, τ and σ, on the fracture surface represents the coefficient of friction μ for the sliding; thus

$$\mu = \frac{\tau}{\sigma} = \frac{(\sigma_1 - \sigma_3) \sin \theta \cos \theta}{\sigma_3 + (\sigma_1 - \sigma_3) \sin^2 \theta}$$

where θ is the angle between the fracture sur-

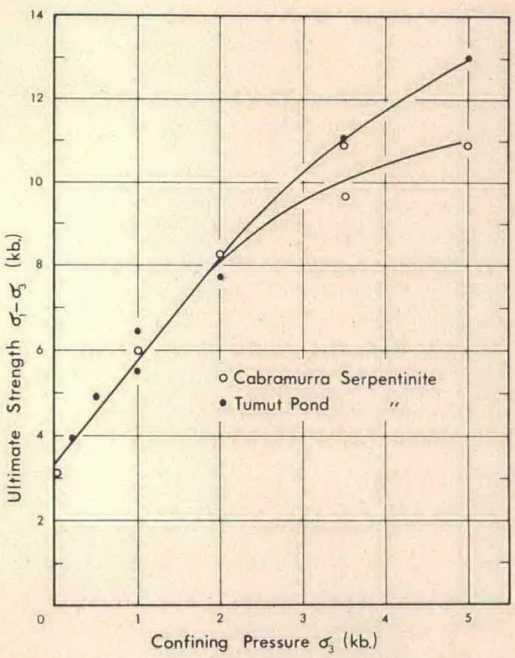

Fig. 2. Plot of ultimate strength, $\sigma_1 - \sigma_3$, against confining presssure, σ_3, for the antigorite-chrysotile serpentinites.

TABLE 1. Summary of Experiments

Temp., °C	Heating Time, hr	Confining Pressure, kb	Ultimate Strength, kb	Mode of Failure	Specimen No.
		Cabramurra Serpentinite			
25		1.0	6.0	Brittle	208
25		2.0	8.2	Transit.	76
25		3.5	9.7	Transit.	57
25		3.5	11.1	Transit.	71
25		5.0	11.1	Ductile	75
150	0.5	3.5	10.2	Transit.	58
250	0.5	3.5	8.5	Transit.	56
350	0.5	3.5	7.9	Transit.	67
400	0.5	3.5	8.0	Transit.	55
400	0.5	3.5	7.0	Transit.	74
450	0.5	3.5	7.2	Transit.	78
475	0.5	3.5	7.7	Transit.	79
500	0.5	3.5	7.2	Transit.	80
500	7.0	3.5	6.9	Transit.	138
513	7.0	3.5	4.3	Brittle	155
527	7.0	3.5	2.9	Brittle	154
550	0.5	3.5	6.3	Brittle	81
550	7.0	3.5	3.1	Brittle	151
575	7.0	3.5	1.1	Brittle	161
600	0.5	3.5	4.0	Brittle	82
600	7.0	3.5	1.1	Brittle	153
630	7.0	3.5	0.9	Brittle	162
650	0.5	3.5	1.2	Brittle	83
675	0.5	3.5	1.7	Brittle	84
700	0.5	3.5	0.7	Brittle	53
*700	0.5	3.5	3.6	Ductile	188
		Tumut Pond Serpentinite			
25		0.2	3.9	Brittle	872
25		0.5	4.7	Brittle	873
25		1.0	5.5	Brittle	874
25		1.0	6.6	Brittle	101
25		2.0	7.8	Brittle	875
230	0.5	1.0	4.9	Brittle	107
275	0.5	1.0	4.9	Brittle	102
454	0.5	1.0	5.3	Brittle	103
500	0.5	1.0	5.3	Brittle	113
550	0.5	1.0	4.0	Brittle	105
600	0.5	1.0	2.7	Brittle	109
*650	0.5	1.0	4.2	Brittle	189
680	0.5	1.0	2.2	Brittle	215
695	0.5	1.0	2.2	Brittle	111
735	0.5	1.0	2.1	Brittle	112
25		3.5	11.2	Transit.	87
25		5.0	13.3	Ductile	88
175	0.5	5.0	12.4	Ductile	114
250	0.5	5.0	10.1	Ductile	89
400	0.5	5.0	9.5	Ductile	90
500	0.5	5.0	8.9	Ductile	91
600	0.5	5.0	7.3	Ductile	104
605	0.5	5.0	7.1	Transit.	127
625	0.5	5.0	4.9	Brittle	100
650	0.5	5.0	2.8	Brittle	128
675	0.5	5.0	1.5	Brittle	129
675	0.5	5.0	1.2	Brittle	98
700	0.5	5.0	0.5	Brittle	96

TABLE 1. (Continued)

Temp., °C	Heating Time, hr	Confining Pressure, kb	Ultimate Strength, kb	Mode of Failure	Specimen No.
		Fidalgo Serpentinite			
25		3.5	8.0	Ductile	119
200	1.0	3.5	6.3	Ductile	135
340	0.5	3.5	5.7	Ductile	120
340	7.0	3.5	2.4	Brittle	173
365	7.0	3.5	2.1	Brittle	172
380	0.5	3.5	2.8	Brittle	137
390	1.0	3.5	1.5	Brittle	125
425	0.5	3.5	3.2	Brittle	122
445	0.5	3.5	2.5	Brittle	118
565	0.5	3.5	0.8	Brittle	121
605	2.0	3.5	0.6	Brittle	141
		Fidalgo Peridotite (partly serpentinized)			
25		3.5	7.9	Ductile	221
200	1.0	3.5	6.9	Ductile	228
300	1.0	3.5	6.4	Ductile	220
355	1.0	3.5	4.9	Transit.	227
405	1.0	3.5	2.8	Brittle	225

* Specimen vented to atmosphere.

face and the applied differential load. The values of μ calculated for the antigorite serpentinites range from 0.68 to 0.91, with a tendency for the Tumut Pond rock to give slightly lower values than the Cabramurra; the Fidalgo rocks also gave lower values (Figure 3). There is also a marked tendency for the value of μ to decrease with increase in confining pressure, as illustrated by the results for the partly serpentinized peridotite from Fidalgo Island given in Figure 3 (this curve was constructed from measurements at various pressures on a single specimen with a shear fracture at 30° to the compression axis).

The decrease in the coefficient of friction with increasing confining pressure for sliding on a fracture surface probably reflects an increasingly important role of processes of crystal plasticity at the sliding surfaces, associated with the transition from brittle to ductile behavior and from a sharply defined fracture surface to a fault zone of finite width. Available evidence [*Bridgman,* 1952; *Haasen and Lawson,* 1958; *Turner et al.,* 1954; *Paterson and Weiss,* 1965] points to the resolved shear stress for crystallographic slip or twinning in metallic and even in complex ionic crystals being relatively insensitive to the normal stress across the glide plane, corresponding generally to values of μ less than 0.1 and often of the order of 0.01 if the variation in yield stress with pressure is interpreted as a frictional effect. Thus, at higher confining pressures, the localized shearing in the faults in the serpentinite after a 'brittle failure' is probably involving slip within serpentine crystals to an increasing degree.

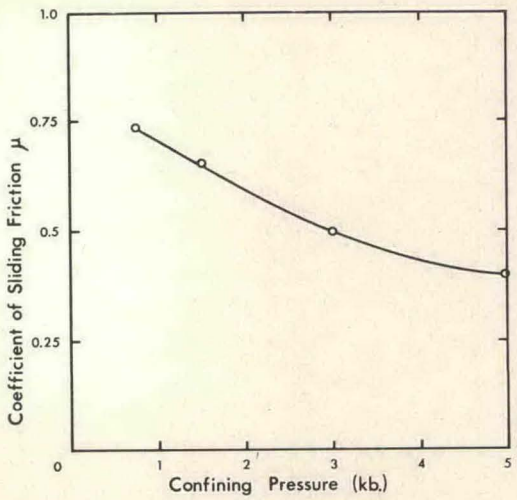

Fig. 3. Coefficient of sliding friction, μ, on shear fracture in partly serpentinized Fidalgo peridotite as a function of confining pressure.

Microscope observations. Study of thin sections shows that in the ductile specimens serpentine grains throughout the deformed zone have become bent or kinked. In the transitional specimens, the faults consist of narrow zones of strongly reoriented serpentine grains; some grains lying outside the faults appear to have been plastically deformed, but the majority of these are adjacent to the fault zones. In the brittle specimens, there is no evidence of plastic deformation outside of a very narrow band of highly oriented serpentine present in places along the fault.

The preferred orientation of the serpentine grains in the fault zones is such that the inclination of the (001) cleavages to the applied load is approximately twice that of the fault (as determined by the average extinction positions of the slow optic directions; (Figure 4). For the sixteen faults examined, the average inclination θ of the fault was 31° (varying from 25 to 39°), whereas the average inclination of the mean extinction position of the slow direction was 61° (varying from 50 to 72°). In a rough estimate, about 80% of the grains in the fault zone extinguish within ±20° of the mean extinction position; further, over 95% extinguish with the slow direction in the same quadrant, so that the field is almost entirely yellow or blue when viewed with the fast direction of the first-order red accessory plate parallel to one or other of the mean extinction positions. The preferred orientation of the serpentine grains in the fault zones has presumably resulted from rotation of grains during plastic or cataclastic deformation, not by recrystallization, since it occurred in tests of a few minutes duration at room temperature.

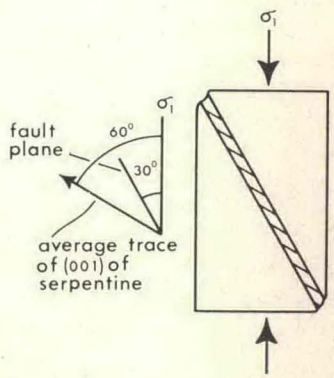

Fig. 4. Diagrammatic sketch of angular relations between maximum principal stress axis, σ_1, fault plane and average trace of (001) in plastically deformed serpentine grains in the fault zone.

High-Temperature Experiments

Stress-strain results—Antigorite serpentinites. The effect of temperatures up to 700°C on the stress-strain curves is illustrated in Figure 5*a* for the Cabramurra serpentinite deformed at 3.5 kb confining pressure and in Figure 5*b* for the Tumut Pond serpentinite deformed at 5 kb; in these tests, the specimens were held at temperature for ½ hour before the load was applied. Two interesting features appear (see Table 1):

1. The ultimate strength, that is, the maximum differential stress reached, decreases by about 35% from 25 to 500°C, whereas in the smaller temperature interval from 500 to 700°C it drops by nearly 90%.

2. At 3.5 kb and 25 to 500°C the stress-strain curves and the appearance of the specimens are typical of the transitional field between brittle and ductile behavior; however, at 600 and 650°C, where greater ductility might normally be expected, the specimens show a brittle type of failure (although this is not always as obvious from the shape of the stress-strain curve as for brittle specimens at low temperatures).

The first effect is shown more clearly in a plot of ultimate strength versus temperature (Figure 6). At all confining pressures, marked drops in strength occur between 500 and 600°C. At 5 kb, the ultimate strength of Tumut Pond serpentinite gradually decreases from 13 kb at 25°C to 7 kb at 600°C but then drops to 0.5 kb at 700°C. The behavior of Cabramurra serpentinite at 3.5 kb is similar, but the rapid decrease in strength begins at a lower temperature (500°C if the duration of prior heating is 7 hours). A rapid decrease in strength of Tumut Pond serpentinite also appears at about 500°C at 1 kb (½-hour heating times), but the ultimate strength only falls from 5 kb at 500°C to 2 kb at 680 to 735°C.

It is noteworthy that the slope of the ultimate strength versus temperature curve (Figure 6) below the 500 to 600°C transition is negligibly small at 1 kb confining pressure but increases as the pressure is increased. The co-

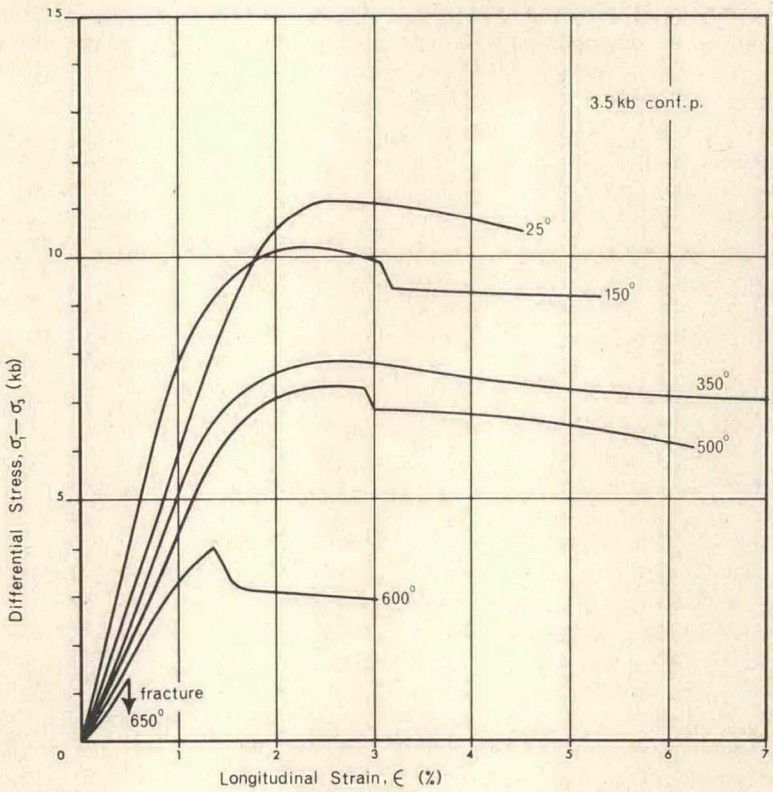

Fig. 5*a*. Stress-strain curves at various temperatures and 3.5 kb confining pressure for Cabramurra serpentinite.

efficient of friction for sliding on the failure surfaces at 1 kb was also approximately constant over the temperature range 25 to 500°C (all specimens tested at 1 kb gave brittle failure). These observations suggest that, although deformation by plastic processes is facilitated by increasing the temperature, the strength is largely unaffected by temperature in the brittle field in accordance with observations of *Handin and Hager* [1958] on some brittle sedimentary rocks.

A marked change in the appearance of the specimens accompanies the 500 to 600°C transition in strength. This is most noticeable at 5 kb confining pressure, where the following was observed. Specimens deformed in a ductile manner with general bulging and distributed deformation at all temperatures below the strength transition. At 600°C faults appeared, although the specimens were still strongly coherent afterwards. A 625°C specimen failed along a single, sharp shear fracture, clearly brittle. At 650 to 700°C, there were also brittle fractures, which tended to lie at small angles to the compression axis; these specimens strongly resembled cylinders fractured in compression at zero confining pressure. The specimens tested at 650 to 700°C were visibly damp when removed from the copper jackets and were lighter in color.

At 3.5 kb confining pressure, specimens deformed at 450 and 475°C were indistinguishable in appearance. They contained a number of fine conjugate shears and one or two large faults in which shearing was distributed over a finite width, and they were slightly barrelled; that is, they were typical of specimens transitional between being brittle and ductile. At 500°C, however, specimens deformed after heating for 0.5 and 7 hours both contained few or no fine conjugate shears, a larger, sharply defined, narrow fault, and a few smaller faults but no distributed deformation, even though the drop in strength from the 450 and 475°C

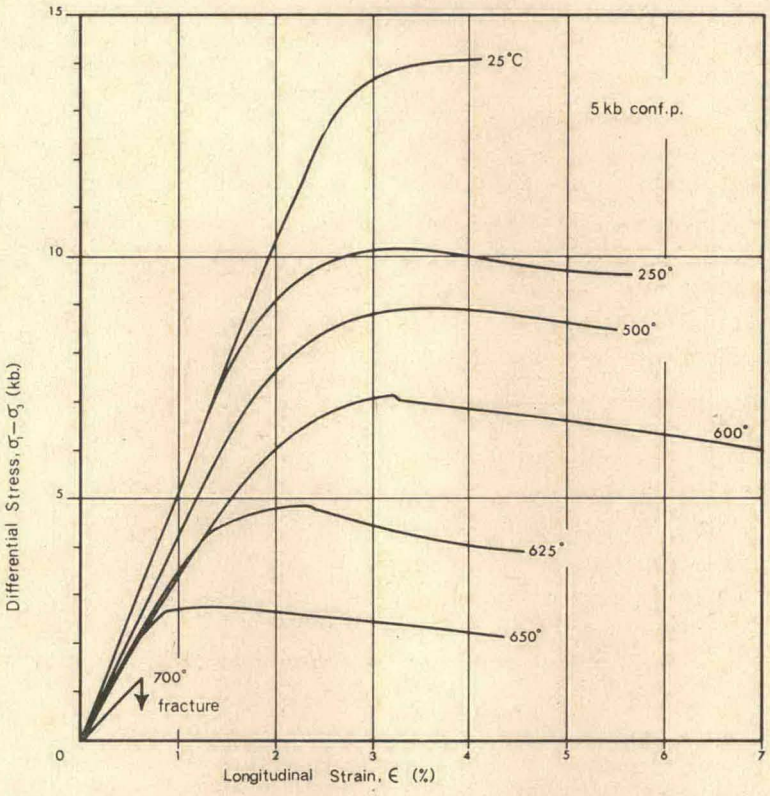

Fig. 5*b*. Stress-strain curves at various temperatures and 5.0 kb confining pressure for Tumut Pond serpentinite.

specimens was less than 0.5 kb. After 7 hours at 510°C, a specimen failed on a single, somewhat irregular shear fracture inclined at 28° to the compression axis, and its ultimate strength was 2.6 kb less than that at 500°C. Thus there is again a rapid onset of brittleness, the first sign of change appearing at 500°C. At 550°C and above, the 3.5 kb specimens were visibly damp on removal from the copper jackets.

In some tests the specimen was vented to atmosphere through a hollow endpiece and piston in order to avoid a rise in pore pressure. A specimen of Cabramurra serpentinite after heating at 700°C and 3.5 kb confining pressure was ductile and gave a continually rising stress-strain curve, with a differential stress of 3.6 kb at 6% strain. This strength is several times that of sealed specimens at 700°C and the ductile behavior is also quite different, sealed specimens at 700°C showing longitudinal splitting similar to that observed in brittle fracture in unconfined compression tests. The specimen suffered a loss in volume after straining due to water from the dehydration being lost to the atmosphere. Another run at 1 kb, on Tumut Pond serpentinite heated for ½ hour at 650°C with the specimen vented, led to a brittle failure at 4.2 kb differential stress (compared with 2.2 kb for a sealed specimen under these conditions).

Stress-strain results—Mesh-texture serpentinites. In the more limited series of experiments on the Fidalgo Island serpentinite at 25 to 600°C and at 3.5 kb confining pressure, stress-strain behavior qualitatively similar to that for the antigorite serpentinites was found, but the marked weakening and embrittlement appeared at a lower temperature (Figure 7*a*). The cross-hatched area in Figure 7*a* includes strengths found after heating times of ½, 1, and 7 hours, the weaker specimens generally having been heated for the longer times. The transition to rapid weakening with increase of temperature occurs at about 300 to 350°C, which is about 200°C lower than the transition for the anti-

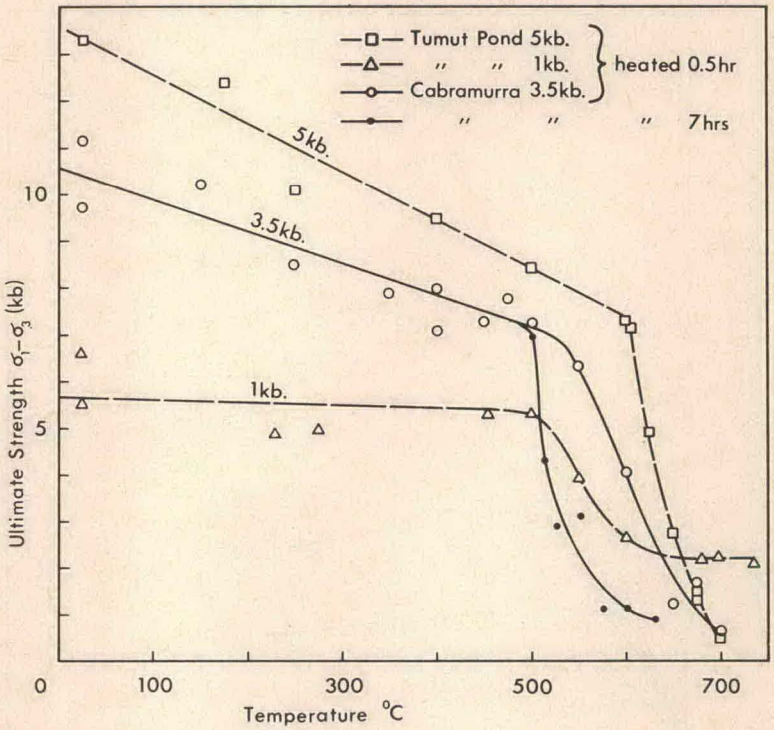

Fig. 6. Ultimate strength of antigorite-chrysotile serpentinites at various confining pressures as a function of temperature. Heating times from ½ hr to 7 hr.

gorite specimens at the same confining pressure. At room temperature, the ultimate strength is about 8 kb, or 2 kb less than for the antigorite serpentinite; at 560°C it is 1 kb, or about one-fifth that of antigorite serpentinite under comparable conditions.

The partly serpentinized peridotite from Fidalgo Island gave very similar results in tests at 3.5 kb confining pressure with 1 hour of heating before deforming. The break in the gradient of strength versus temperature occurred at about 300°C (Figure 7*b*).

The brittle-ductile changes that accompany the changes in strength with increasing temperature are illustrated very clearly in the mesh-texture serpentinite. At room temperature, failure occurred along a single shear fracture running through a narrow zone of distributed deformation (Figure 8), the appearance suggesting behavior transitional between brittle and ductile. Increase of temperature to 200°C leads to an increase in ductility, the zone of shearing increasing in width and the fracture being absent. After ½ hour at 340°C (Figure 8), a specimen was quite ductile, deforming to a regular barrel-shape without local shearing. At higher temperatures, and after 7 hours at 340°C, all specimens were brittle (Figure 8, 375°C, 400°C). Dampness of the specimen was first visible after an experiment involving heating for 1 hour at 385°C. The 560 and 600°C specimens were strongly reacted and very damp when removed from the jackets.

Thus, compared with the antigorite serpentinite, the mesh-textured, chrysotile-lizardite serpentinite is more ductile and slightly weaker at low temperatures. However, the weakening and embrittlement with increase in temperature set in at considerably lower temperatures than in antigorite serpentinite—at about 300°C instead of about 500°C at 3.5 kb confining pressure.

Microscope and X-ray examination. Thin sections of representative high-temperature specimens were studied for mineralogical and textural changes from the heating, as well as for details of the faults. However, the X-ray

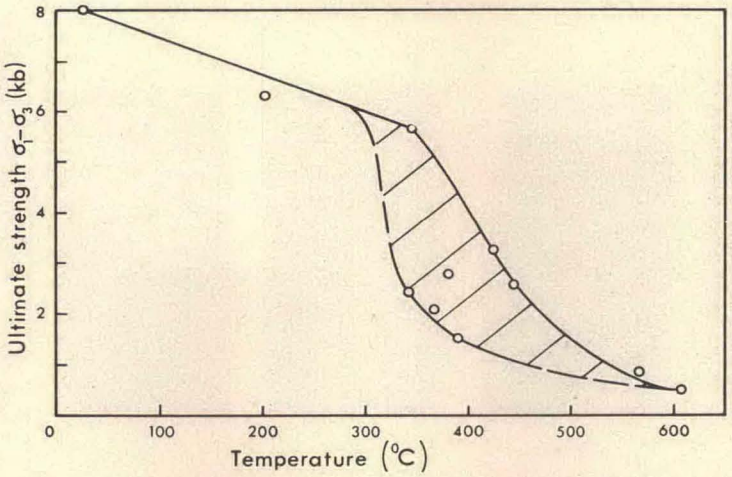

Fig. 7*a*. Ultimate strength of mesh-texture serpentinite from Fidalgo Island as a function of temperature at 3.5 kb confining pressure.

diffractometer was used to identify the new mineral phases because of their fine grain size; the results are summarized in Table 2.

A prominent reflection, corresponding to 11.3 A and of about the same sharpness as the normal 7.3 A serpentine reflection, was observed on diffractometer charts from specimens 92 and 100, heated at 5 kb for 30 minutes at 600 and 625°C, respectively. *Brindley and Zussmann* [1957] observed a broad reflection decreasing from 14 to 10 A in serpentines heated at 500 to 750°C and attributed it to mixed layer sequences of a chlorite-like unit and a forsterite unit. Possibly such a mixed-layer sequence is responsible for the present 11.3 A reflection, but its restriction to a narrow temperature range and lack of broadening do not correspond exactly to Brindley and Zussmann's case.

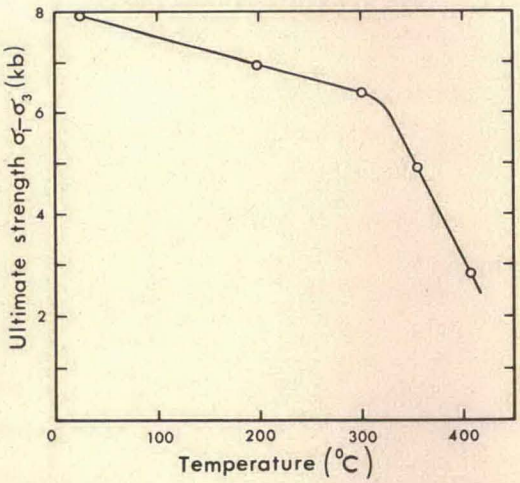

Fig. 7*b*. Ultimate strength of partly serpentinized peridotite from Fidalgo Island as a function of temperature at 3.5 kb confining pressure. Heating times of 1 hour.

Microscope examination revealed little change apart from strain effects up to temperatures 25 to 75°C beyond the beginning of the high-temperature embrittlement and weakening. After experiments at higher temperatures, when the specimens became visibly damp, mineralogical change was evidenced by the presence of 5- to 50-μ grains of olivine and talc, concentrated along the boundaries of the serpentine grains and, in the Cabramurra serpentinite, pre-existing olivine grains. The new grains are elongate (Figure 9) and, in the case of olivine, often in optical continuity with the contiguous original olivine grains. In orientation, the new olivine grains bear no apparent epitaxial relation to the serpentine grains or special relation to the specimen axis. Highly comminuted material along faults in some specimens deformed at temperatures within the olivine stability field has a high refractive index, but it could not be identified.

To check on the composition of the olivine synthesized by dehydration of serpentine in the experiments, we heated specimens of Tumut Pond and Fidalgo serpentinites, which originally

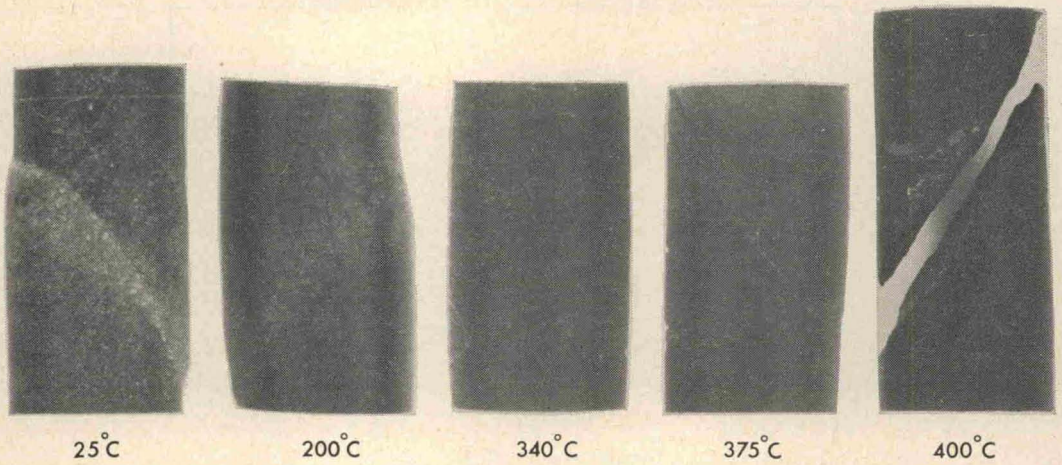

Fig. 8. Cores of Fidalgo serpentinite 1 cm in diameter deformed at 3.5 kb at various temperatures are ductile to 340°C, brittle at 375 and 400°C, where weakening has set in.

are free of olivine, for 2 hours at 675°C and 3.5-kb confining pressure and prepared concentrates of the synthesized olivine after grinding. Pure olivine fractions could not be obtained for chemical analysis because of the fine grain size, so the X-ray method of *Hotz and Jackson* [1962] was used. Assuming the relation between lattice spacing and composition determined experimentally by Hotz and Jackson for their material, we determined the composition of the olivine formed in the Tumut Pond specimen to be Fo_{96} (the measured angle between (062) olivine and (220) LiF peaks being $2.78 \pm 0.02°$), while the olivine from the Fidalgo specimen

TABLE 2. Phases Recognized (Excluding Magnetite) by X-ray and Optical Examination of Starting Material and Experimental Specimens

Temperature, °C	Heating Time, hr	Confining Pressure, kb	Olivine	Talc	Serpentine	Brucite
			Cabramurra Serpentinite			
500	7.0	3.5	X		X	
513	7.0	3.5	XX*		X	
552	7.0	3.5	XX		X	
575	7.0	3.5	XX	X	X	
600	7.0	3.5	XX	X	X	
630	7.0	3.5	XX	X		
650	0.5	3.5	XX	X	X	
			Tumut Pond Serpentinite			
500	0.5	5.0			X	
600	0.5	5.0			X	
625	0.5	5.0			X	
650	0.5	5.0			X	
675	0.5	5.0	X	X	X	
			Fidalgo Serpentinite			
200	1.0	3.5			X	X
340	7.0	3.5			X	X
363	7.0	3.5			X	X
565	0.5	3.5	X		X	

* Indicates neocrystalline olivine observed in thin section.

Fig. 9. Neocrystalline olivine needles in optical continuity with relict olivine grain in matrix of serpentine. Cabramurra serpentinite number 151 deformed after 7 hours heating at 550°C, 3.5 kb confining pressure.

gave a nominal composition of Fo_{102} (peak difference 2.69 ± 0.03°). These results probably indicate that the olivine formed has a high forsterite content, but they also show that the (062) spacing does not vary with relative forsterite-fayalite content in the same way as in the olivines studied by Hotz and Jackson. Possibly the olivine produced hydrothermally contains smaller amounts of elements having large ionic radii, such as Ca^{++}, than that crystallized at the much higher temperatures of magmas. Small amounts of such ions in the Mg-Fe lattice sites could seriously affect the lattice spacing relations of Hotz and Jackson, so that the forsterite contents determined in hydrothermal olivine by the X-ray method may be spuriously high.

Discussion of the Experimental Results

Brittle-Ductile Relations

It is common experience in experimental deformation studies that rocks which are brittle under atmospheric conditions or at relatively low temperatures and pressures may become ductile at higher temperatures or higher confining pressures, due, in the first case, to the temperature lowering the yield stress to less than the fracture stress and, in the second, to the pressure raising the fracture stress to more than the yield stress. The striking feature of the serpentinite experiments with sealed specimens is the sharp transition from ductile to brittle behavior that occurs upon *increase* of temperature, even at the relatively high confining pressure of 5 kb.

The brittle, transitional, and ductile fields of temperature and confining pressure are depicted in Figures 10*a* and *b* for the antigorite and mesh-texture serpentinites, respectively, although because of incomplete data the positions of the boundaries are somewhat indefinite, especially the nearly vertical boundary of the high-temperature brittle field for the mesh-texture serpentinite.[2] The subhorizontal part of the brittle field boundary corresponds to the usual transition from ductile to brittle behavior as the pressure is lowered. The steeply rising part of the boundary corresponds to the transition to brittle behavior that may occur at high pressure when the temperature is raised sufficiently. This is the transition that is of novel interest and the mechanism of which we now discuss.

Mechanism of High-Temperature Embrittlement and Weakening

The experiments point strongly to the high-temperature embrittlement and weakening of the serpentinite being intimately related to de-

[2] The criterion used here to distinguish brittle from ductile behavior is that brittle fracture takes place without accompanying plastic deformation as determined from examination of thin sections. Transitional specimens are fractured but coherent and, in thin section, show evidence of distributed flow within or near the fault zone. Ductile specimens deform predominantly by distributed plastic flow; they may contain fine conjugate shears which, however, contribute little to the total strain. The shapes of the stress-strain curves at room temperature tend to be rounded and continuous for ductile specimens and, for brittle specimens, to drop sharply at strains of a few per cent; however, at high temperatures brittle and ductile behavior may not be reliably distinguished on this basis.

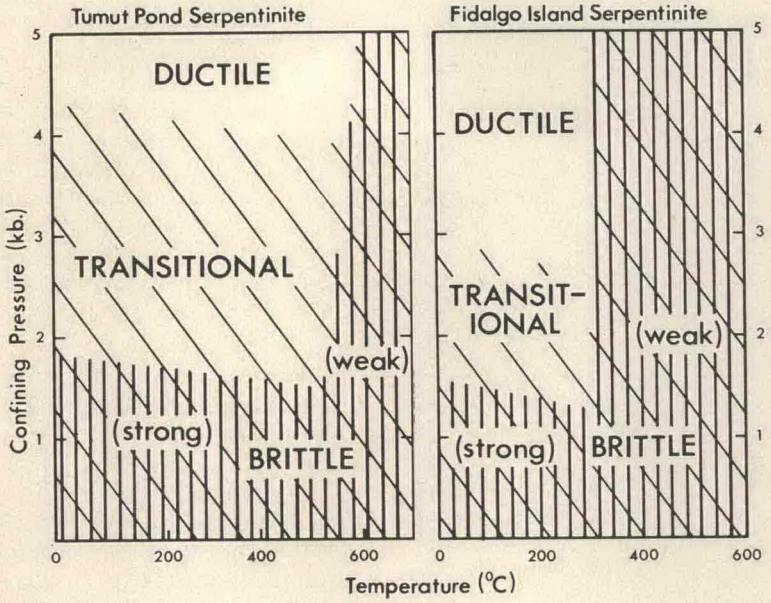

Fig. 10. Brittle, transitional, and ductile regions of pressure-temperature field for antigorite-chrysotile serpentinite (*left*) and mesh-texture serpentinite (*right*). Location of boundaries approximate.

hydration reactions, both because the temperatures are appropriate (see below) and water is observed to be present after the higher-temperature experiments in which the effect is strongly developed. There are three possible mechanisms by which the dehydration may lead to this effect.

1. *Pore pressure.* The pressure of the water (and any other gases such as CO_2) released into pores and grain boundaries will reduce the effective confining pressure, thus leading to embrittlement and to some weakening (see introduction). Since the water will be first released at nucleation sites on grain boundaries throughout the specimen (the new phases are seen to be distributed along the grain boundaries), it should readily pervade the whole specimen, filling any original pores and creating new ones in the grain boundaries.

2. *Loss of cohesive strength.* After an appreciable amount of reaction, leading to the presence in grain boundaries of new phases and newly formed pores needed to accommodate the released water, the solid framework of the specimen will no longer be the same and there will probably be a weakening of its 'cohesive strength,' especially due to new pores. The absence of a marked drop of load upon brittle failure at temperatures well above the onset of the transition could be the result of such a disintegration of the structural framework.

3. *'Water weakening.' Griggs and Blacic* [1964, 1965] found that quartz crystals containing small amounts of water in the structure were very weak and ductile at temperatures down to 400°C and a strain rate of 8×10^{-6} sec^{-1}, conditions under which dry quartz has exceptionally high strength. The serpentinites in our experiments become embrittled rather than more ductile, and therefore in this respect the weakening is apparently not the same as the water-weakening effect. However, Griggs and Blacic's experiments suggest the possibility of an analogous weakening in the serpentine grains themselves or in the neocrystalline phases at the grain boundaries. In our experiments this could not be distinguished from a loss in cohesive strength and will not be discussed further.

The two mechanisms of weakening to be discussed are, therefore, loss of cohesion and reduction in effective confining pressure due to pore pressure. The cohesive strength, τ_0, measured at room temperature is 0.9 kb, whereas at 700°C the minimum ultimate strength is 0.5

kb, corresponding to $\tau_0 = 0.15$ kb, if we assume pore pressure to be equal to confining pressure and the angle of internal friction, ϕ, to be unchanged. It is improbable that reduction in τ_0 could account for the whole of the observed weakening, however, as the fracture angles in the weakened specimens are $\theta = 30°$, corresponding to $\phi = 30°$ in the other term of the Coulomb-Navier expression. Furthermore, the vented specimen at 700°C and 3.5 kb has a strength several times that of a sealed specimen under the same conditions, which indicates that pore pressure is required to effect the observed weakening and embrittlement.

It is not possible in the present work to distinguish unambiguously between the roles of pore pressure of water and loss of cohesion upon dehydration, but, in order to illustrate the nature of some of the considerations involved, we shall attempt to analyze the Cabramurra serpentinite at 3.5 kb, for which the data at longer times were obtained. The solid curve in Figure 11 gives the water pressure P_w at equilibrium as a function of temperature for the reaction

5 serpentine = 6 forsterite + talc + 9 H_2O

when the total pressure P_s in the solid phases is 3.5 kb. The method by which we calculated P_w from the equilibrium curve for $P_w = P_s$, using the data of *Pistorius* [1963], is given in Appendix A. Thus at any given temperature below that for which $P_w = 3.5$ kb, dehydration of jacketed serpentine held at a confining pressure of 3.5 kb can proceed until the pore pressure of water reaches the value of P_w given by this solid curve. We shall assume that this curve applies to the Cabramurra serpentinite, except for a slight shift along the temperature axis, so that the beginning of dehydration corresponds to the beginning of the marked strength loss near 500°C.

Equation 1 predicts a loss of shear strength of $P_w \tan \phi$ in a brittle, permeable material because of the introduction of a pore pressure P_w; from Appendix B, the corresponding decrease in $\sigma_1 - \sigma_3$ would be $2 \sin \phi/(1 - \sin \phi)\ P_w$, or $2.4P_w$ with the constants from (2), that is, 8.4 kb for $P_w = 3.5$ kb. However, such a calculation cannot be applied directly to the Cabramurra serpentinite because it is not completely brittle at the inception of dehydration at 3.5 kb confining pressure and its strength is prob-

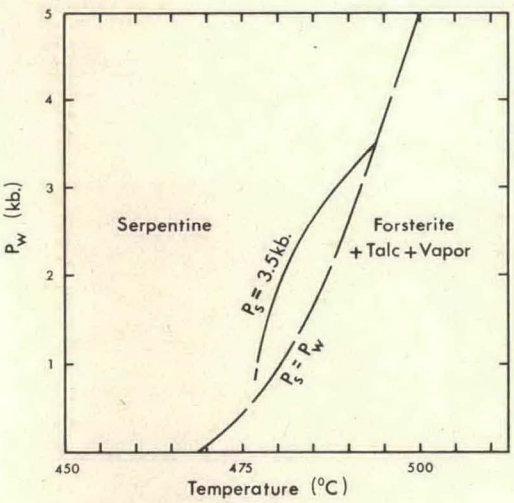

Fig. 11. *P-T* equilibrium boundary for $P_w = P_s$ [from *Pistorius*, 1963] for serpentine dehydration (dashed line) and P_w-*T* boundary calculated for confining pressure $P_s = 3.5$ kb (solid line).

ably not a linear function of pressure. The effect of confining pressure on the ultimate strength has not been determined at temperatures just below the dehydration range, but it can be assumed to be represented approximately by the broken curve marked 500°C in Figure 12 since the point Q at 3.5 kb has been measured and measurements on the similar Tumut Pond rock show that the strength at 1 kb is almost unchanged up to temperatures just below the dehydration range. Thus, the loss of strength at 3.5 kb on heating from room temperature to just below the dehydration range probably corresponds to a more marked bending over of the $\sigma_1 - \sigma_3$ versus σ_3 curve than at room temperature (expressed as a sharper curvature of the Mohr envelope in a Mohr diagram).

We now assume that the 'effective pressure' concept can be generalized somewhat to apply to porous materials transitional between brittle and ductile, that is, that in the presence of a pore pressure p the ultimate strength of such a material is given by the point with abscissa $\sigma_3 - p$ on the $\sigma_1 - \sigma_3$ versus σ_3 curve. Then, with increasing water pressure from dehydration, the ultimate strength of the serpentinite will tend to decrease along a path close to the 500°C curve in Figure 12. The small amount of dehy-

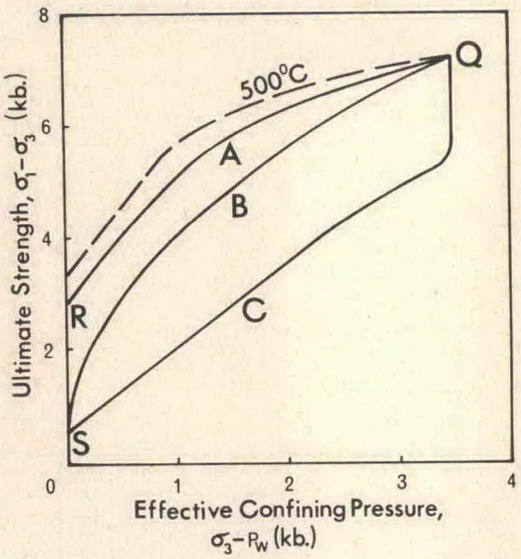

Fig. 12. Suggested interpretations of decrease in ultimate strength with increase in temperature, associated with decrease in effective confining pressure due to dehydration. Points Q and S are experimentally determined at $\sigma_3 = 3.5$ kb, with $P_w = 0$ at 500°C and $P_w = 3.5$ kb at 700°C, respectively. The broken curve represents the approximate ultimate strength at 500°C with $P_w = 0$. Curve A gives the strength loss with rising water pressure on further heating, assuming small loss of cohesion as far as point R where $P_w = 3.5$ kb, and further weakening to point S due to loss of cohesion as dehydration proceeds isothermally. Curve B represents strength loss under conditions of inequilibrium. Curve C represents the possibility of a large decrease in cohesive strength at an early stage of dehydration, before the effective confining pressure drops appreciably.

dration necessary to fill existing pores with water at 3.5 kb probably leads to some loss of cohesion ('cohesion' being proportional, as before, to the $\sigma_3 = 0$ intercept of the $\sigma_1 - \sigma_3$ versus σ_3 curve), so that an actual path such as A (Figure 12) should be followed under equilibrium conditions, reaching R at the temperature at which P_w reaches 3.5 kb. On further slight increase in temperature, dehydration will, given sufficient time, go to completion isothermally while the strength falls from R to S (loss of cohesion) because of the changes in the structure of the specimen. In practice, departure from equilibrium can arise from (*a*) sluggishness of the dehydration reaction or (*b*) lack of permeability in a material of low porosity, so that the water pressure is not fully 'effective,' and the strength is more likely to follow a path such as B in Figure 12, the temperature having been raised substantially before point S is reached. Such a path is probably consistent with the present observations since, although full water pressure should be reached in a 25°C interval of temperature increase (Figure 11), the strength decrease is spread out over a much greater temperature range.

An alternative path C (Figure 12) represents the possibility that the first stages of dehydration effect a drastic reduction in the cohesion before the effective pressure is appreciably decreased, after which the strength follows a Coulomb-Navier line reaching a point in the neighborhood of S when the water pressure reaches 3.5 kb after a 25°C rise in temperature. The observations do not appear consistent with the latter path since the strength is still relatively high at a stage when the specimen is already visibly damp and the effective pressure may be assumed to be much reduced. We therefore conclude that the effect of pore pressure of water is probably predominant in the earlier part of the strength reduction, after which the decrease in cohesion becomes important. However, the following reservations must be made:

(*a*) There are two ways in which the strength testing may introduce departure from equilibrium in the specimen. First, the application of a compressive differential stress will tend to increase the pressure of fluid in the pores and, second, local dilatation from the propagation of small cracks in the fault zone at the moment of failure (cf. *Brace* [1964]) will tend to decrease the pore pressure. Both effects would be reduced at slower testing rates and are unlikely to be important in geological situations where the rate of build-up of stress is probably slow enough for dehydration or rehydration reactions to keep the water pressure at the equilibrium value.

(*b*) The calculation has been based on data for dehydration of pure magnesian serpentine. However, in the serpentinite rocks, variations in purity and in the nature of other phases present may seriously affect the dehydration data. Comparison of the theoretical transition in Figure 12 with the measurements on the Tumut Pond or Fidalgo rocks (Figures 6 and 7) shows wide discrepancies in temperature, in view of which the degree of agreement for the

Cabramurra rock may be fortuitous. This leads us to more detailed chemical consideration.

Dehydration reactions. Experimental studies of the dehydration of serpentine to yield forsterite and talc have mainly involved the chrysotile form of serpentine. There is some evidence that the antigorite form or serpentines containing some aluminum may be stable to somewhat higher temperatures [*Gillery,* 1959], but P_w equilibrium curves are not available. However, when brucite is present the reaction

$$\text{serpentine} + \text{brucite} = 2\ \text{forsterite} + 3\ H_2O$$

has been shown to proceed at temperature 50 to 75°C or more lower at a given pressure than the dehydration of pure serpentine [*Bowen and Tuttle,* 1949; *Pistorius,* 1963]. Since the Fidalgo rocks contain some brucite and have not yielded talc in the experiments (Table 2), this reaction may, at least in part, explain the much lower temperature of the brittle transition in these rocks, although the whole discrepancy of some 200°C calls for additional explanation, such as dependence of equilibrium relations on the serpentine phase or on other undetected phases participating in the reaction or on the presence of impurities like FeO. The results for Tumut Pond serpentinite at 5 kb give a transition temperature appreciably higher than for the dehydration of pure serpentinite. Again, impurities may be important. At temperatures of 650 to 750°C, talc dehydration reactions will contribute additional water [*Bowen and Tuttle,* 1949].

Other aspects. There are several indications that equilibrium is not readily attained in experiments of up to 7-hours duration. The transitional parts of the strength curves for Cabramurra and Fidalgo serpentinites (Figures 6 and 7*a*) are steeper and occur at lower temperatures after 7 hours heating than after ½ hour. Even at higher temperatures, the material does not completely react in the times used. A gradual build-up of the water pressure is also reflected in measurements on the coefficient of friction for sliding on fracture surfaces. The results in Figure 13 refer to a specimen of Tumut Pond serpentinite in which a shear fracture was produced after ½ hour heating at 600°C; the stress needed for sliding on this fracture is plotted as a function of succeeding time, probably showing the effect of rising water pressure. In all specimens deformed at temperatures above the transition, the stress for sliding on a single fracture surface was found to be much less than that in similar experiments below the transition.

Results on the partly serpentinized Fidalgo peridotite (Figure 7*b*) show that the high-temperature embrittlement and weakening can occur when only part of the rock consists of a mineral that will dehydrate. Clearly the effect can be expected to be of wide importance, although the results in this paper show that to reconcile measured effects with prediction from phase equilibrium studies may require much more detailed work on the latter. We now consider some geological implications of the serpentine work. It must be borne in mind that the experiments refer to completely sealed specimens and that, in practice, the behavior may be modified if water can escape from the system (as shown by the experiment on a vented specimen mentioned above).

Geological Significance of Results

Tectonic Intrusion of Alpine Serpentinite

The experiments have shown that the strength of serpentinites is as great as that of most rocks at temperatures below a limit somewhere in the range 300 to 600°C, the position of this limit apparently being fixed by the first appearance of an appreciable water pressure in equilibrium with the serpentine. The cohesive strength, τ_0,

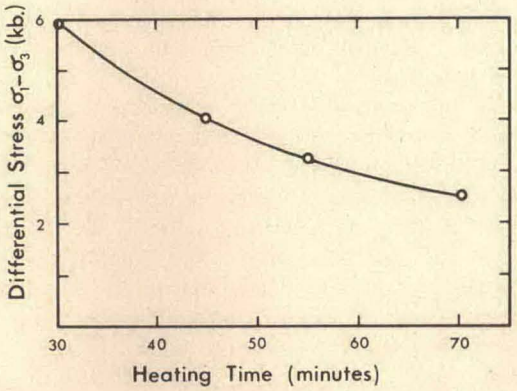

Fig. 13. Differential stress for sliding on fracture surface in Tumut Pond serpentinite as a function of time at 600°C.

and the coefficient of internal friction for brittle failure at these temperatures are, in fact, greater than for most sedimentary rocks [*Handin and Hager,* 1957]. The coefficient of friction for sliding on a fracture surface is also at least as great as for other rocks [*Jaeger,* 1959; *Handin and Stearns,* 1964]. Although these conclusions are based on short-time tests, the same relation of properties can be expected in general to hold at longer times, since the dehydration temperatures of serpentine and related minerals are known to correspond to conditions close to equilibrium. Thus, the experimental conclusions should be broadly applicable under geological conditions.

The solid intrusion process of *Hess* [1955] (see introduction above) requires the serpentinite to fracture and then slide on the fracture surfaces at a stress difference below that for yielding or fracture in the surrounding rocks. However, the present work suggests that under normal conditions in the upper part of the crust the strength and friction relations make such a process impossible unless the surrounding rocks are igneous or metamorphic, or are strong sedimentary rocks, such as dolomite or silica-cemented quartzite [*Griggs et al.,* 1960; *Handin and Hager* 1957; *Handin et al.,* 1963]. The same difficulty confronts the intrusion hypothesis of *Bowen and Tuttle* [1949], which involves flow in a serpentinite shell on an alpine peridotite body (cf. the similar notion of *Orowan* [1964] that serpentine can act as a 'lubricant' on account of its supposed weakness). The preservation of mesh texture in alpine serpentinites is also evidence against intensive plastic deformation since, in the the experiments, 20% strain rendered mesh texture no longer easily recognizable.

These difficulties with intrusion models are met if the serpentinite is at a temperature at which an appreciable water pressure is in equilibrium with its mineral assemblage. This temperature is in the range 300 to 600°C, depending on composition and total pressure (depth of burial). The water pressure can be caused by partial dehydration of the serpentinite if water is not being lost at too great a rate to the surroundings (permeability is probably low as long as the total pressure is somewhat greater than the water pressure). The strength of the serpentinized parts of the body will then be low compared with that of surrounding rocks; brittle fracture and subsequent sliding on fracture surfaces will be possible in the serpentinite at low shear stresses because of the weakening effect of the pore pressure of water, as demonstrated in the experiments. Also, general plastic deformation will not occur because of the mode of failure being brittle fracture, which will be confined to a pattern of localized fracture zones depending on the nature of the external constraints. Therefore, any original mesh texture can be preserved, provided that dehydration has not gone to a point of obliterating it. We conclude that solid intrusion of serpentinized bodies can occur at the temperatures mentioned by sliding on discrete fracture surfaces, much as envisaged by *Hess* [1955], but with the provision that fluid pressure lowers the effective normal stress across the fractures sufficiently for the sliding to occur at low shear stresses.

Alpine serpentinites have often been described as being highly sheared in comparison with the country rocks [*Lapham and McKague,* 1964]. This is consistent with the model just described, although it is not necessary for faulting to occur throughout the serpentinite mass, especially since small temperature gradients may produce large gradients in water pressure and, consequently, large gradients in strength. In light of this, cases in which the geological evidence has apparently precluded tectonic intrusion of serpentinite might be reconsidered. For example, the serpentinite breccias of Queensland [*Wilkinson,* 1953] may have originated from faulting of a mass of serpentinite which was in a brittle and weak condition because of high water pressure from dehydration. No olivine is now present which might have been produced by dehydration but this olivine may have been re-serpentinized during cooling; it may be difficult to recognize the regenerated serpentine as such. The schistose phase and angular fragments noted by Wilkinson have their parallels within the fault zones of the weak and brittle experimental specimens. Further, the presence of well-defined mesh textures is compatible with the present model. Therefore, the brecciation might well have occurred during intrusion under conditions in which the serpentinite is weakened and embrittled as a result of partial dehydration.

Role of Serpentinite in Tectonics[3]

In light of the previous section, the widespread and characteristic occurrence of serpentinized bodies in island arcs and alpine mountain chains suggests that the serpentine may play an important part in the tectonic development of such regions, involving especially the oceanic crust and upper mantle. Various authors have suggested that serpentinite is present as a layer at the base of the oceanic crust (cf. *Hess* [1955]) or it may be a minor constituent of a peridotite shell at shallow levels in the upper mantle (*Birch* [1961] has shown that seismic velocities would be consistent with this). If, at a time of tectonic activity, the isotherms rise nearer the surface or the lower crustal and upper mantle rocks are depressed to hotter regions, partial dehydration and consequent weakening and embrittlement of the serpentine-bearing rocks may occur when the appropriate temperature in the region 300 to 600°C is reached. Provided that the water is not lost, this will greatly facilitate cataclastic deformation in the hot zone, so that not only will relative movement of adjacent rock masses occur easily but this activity will be confined to the hot zones because the drier rocks outside these zones will be much stronger. Thus, the tectonic activity can be intense and local, as is characteristic of a mountain chain, in the presence of moderate thermal gradients.

The observation of brittle failure at shear stresses low compared with the total pressure in dehydrating serpentinite suggests that this may be an important seismic focal mechanism in the tectonically active regions just discussed, at least in the lower crust and perhaps in the upper mantle. *Griggs and Handin* [1960], in discussing the problem that faulting by brittle fracture would normally require prohibitively high shear stresses at all but the shallowest depths, have already suggested as one possibility that a pore pressure of water released in a dehydration reaction may reduce the frictional term and make brittle fractures possible at greater depths. The serpentinite experiments lend support to this suggestion. Therefore, in regions where serpentinite is playing a predominant part in the tectonic processes, we may expect that, with increasing depth, the frequency of earthquakes should at first decrease, corresponding to the increase in ductility with pressure at lower temperatures and then markedly increase when the dehydration zone is reached. This type of earthquake mechanism may also be of somewhat more general occurrence; thus, at greater depths or in other regions, other minerals such as micas or amphiboles may similarly provide a pore pressure of water by dehydration. Perhaps, the concept could even be extended to deep-focus earthquakes if the mantle material there contains a phase, effectively devoid of shear strength (through being very near its melting point or for some other reason), which functions as a fluid phase between the stronger phases present; then the nonhydrostatic stresses would be supported by the stronger phases but cataclastic or brittle fracturing might occur if the weak phase plays a part analogous to that of the water in the serpentinite.

[3] *Footnote added in proof.* H. C. Heard and W. W. Rubey will discuss other aspects of the role of serpentinite in tectonics in a forthcoming paper.

Appendix A

We need to calculate the equilibrium water pressure P_w for the serpentine dehydration reaction as a function of temperature when the total pressure P_s in the solid phases is fixed and $P_w < P_s$. For this, we have used the following approximate expressions derived and tested by *Greenwood* [1961]:

$$P_w = \tfrac{1}{2}\left[\frac{(\Delta V_s)^2 \dfrac{\partial V_w}{\partial P_w}}{V_w^3}\right] P_s^2 - \frac{\Delta V_s}{V_w} P_s + C_3$$

(the notation is Greenwood's except for P_w and V_w, the volume of water released by the reaction). The constant, C_3, was evaluated at different points on the equilibrium P-T curve for $P_w = P_s$ of *Pistorius* [1963], and V_w and $\partial V_w/\partial P_w$ were estimated using the P-V-T data for water of *Holser and Kennedy* [1959]. Another approximate expression,

$$P_w = P_s - \Delta T \frac{\Delta S}{V_w} - \frac{(\Delta T)^2}{2}\left[\frac{\Delta S^2}{V_w^3}\left(\frac{\partial V_w}{\partial P_w}\right)_T - \frac{\Delta S}{V_w^2}\left(\frac{\partial \Delta S}{\partial P_w}\right)_{P_s,T} - \frac{\Delta C_p}{V_w T}\right]$$

which can be derived from Greenwood's relations, may also be used when P_w is near P_s;

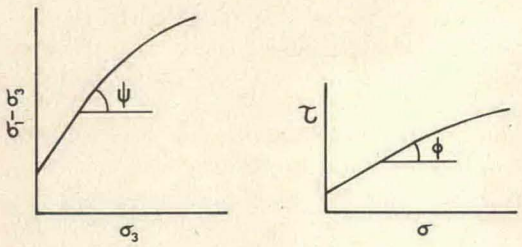

Fig. 14. Failure envelopes on $\sigma_1 - \sigma_3$ versus σ_3 and τ versus σ (Mohr envelope) plots. ψ and ϕ, respectively, are slopes of the envelopes.

the coefficients in the second and third terms can be evaluated with the aid of his expressions 5 and 21.

The equilibrium P_w-T curve thus calculated (solid line in Figure 11) is probably unreliable at the lower temperatures because of the uncertainty in the slope of Pistorius's curve in this region, and it is uncertain to some extent in view of the discrepancies between the data of Pistorius and of Bowen and Tuttle. Further error can arise from the approximations used and from extrapolation of Holser and Kennedy's data for water. However, because of the steepness of the P-T boundary for dehydration of serpentine, the effect of these uncertainties is unimportant in the present situation.

Appendix B

The experimental results on the effect of pressure have been presented in the form of plots of $\sigma_1 - \sigma_3$ versus σ_3 because these are the measured quantities and this form of presentation is most nearly free of implied interpretation. However, it is often useful in discussion to represent the results in a Mohr diagram, especially if the Mohr envelope is to be considered. The Mohr envelope is an alternative representation of the experimental results, and it can be plotted directly using the following relations:

If $\sigma_1 - \sigma_3$ and σ_3 are the coordinates of a given point on the curve connecting the experimental results in the $\sigma_1 - \sigma_3$ versus σ_3 plot and $\tan \psi$ is the slope at this point (Figure 14), the corresponding point in the Mohr envelope is

$$\tau = \frac{(\sigma_1 - \sigma_3)(1 + \tan \psi)^{1/2}}{2 + \tan \psi}$$

$$\sigma = \sigma_3 + \frac{(\sigma_1 - \sigma_3)}{2 + \tan \psi}$$

and the slope of the Mohr envelope at this point is $\tan \phi = \tan \psi / 2(1+\tan \psi)^{1/2}$.

In the special case when the experimental results obey the linear relation

$$\sigma_1 - \sigma_3 = a + \sigma_3 \tan \psi$$

the Mohr envelope is the straight line (Coulomb–Navier relation)

$$\tau = \tau_0 + \sigma \tan \phi$$

where

$$\tau_0 = \frac{a}{2(1 + \tan \psi)^{1/2}}$$

$$\tan \phi = \frac{\tan \psi}{2(1 + \tan \psi)^{1/2}}$$

Conversely, this straight-line Mohr envelope corresponds to the following line in the $(\sigma_1 - \sigma_3)$ versus σ_3 plot:

$$\sigma_1 - \sigma_3 = \frac{2 \cos \phi}{1 - \sin \phi} \tau_0 + \frac{2 \sin \phi}{1 - \sin \phi} \sigma_3$$

The above expressions may be modified to take account of pore pressure, p, by substituting for σ_1 and σ_3 the effective stresses, $\sigma_1 - p$ and $\sigma_3 - p$.

Acknowledgments. The manuscript was critically reviewed by Professors D. T. Griggs and W. W. Rubey. The sample of partly serpentinized peridotite from Fidalgo Island was kindly supplied by Mr. Marshall Huntting of the Washington State Division of Mines. We are also grateful to Mr. W. van Barneveld and to members of the workshops of the Research School of Physical Sciences for much work in constructing and assembling the apparatus and to Professor J. C. Jaeger for continued encouragement of research in experimental deformation.

References

Birch, Francis, The velocity of compressional waves in rocks to 10 kilobars, *J. Geophys. Res., 66,* 2199–2224, 1961.

Bowen, N. L., and O. F. Tuttle, The system MgO-SiO_2-H_2O, *Bull. Geol. Soc. Am., 60,* 439–460, 1949.

Brace, W. F., Brittle fracture of rocks, in *State of Stress in the Earth's Crust,* edited by W. R. Judd, American Elsevier Publishing Company, New York, 1964.

Bridgman, P. W., *Studies in Large Plastic Flow and Fracture,* 326 pp., McGraw-Hill Book Company, New York, 1952.

Brindley, G. W., and J. Zussmann, Thermal transformation of serpentine minerals to forsterite, *Am. Mineralogist, 42,* 461–474, 1957.

de Roever, W. P., Sind die alpinotypen Peridotitmassen vielleicht tektonisch verfrachtete Bruchstücke der Peridotitschale?, *Geol. Rundschau, 46,* 137–146, 1957.

Dietz, Robert, Ocean-basin evolution by sea-floor spreading, chapter 10, *Continential Drift,* Academic Press, New York, 1962.

Fyfe, W. S., F. J. Turner, and J. Verhoogen, Metamorphic reactions and metamorphic facies, *Geol. Soc. Am. Mem., 73,* 259 pp., 1958.

Gillery, F. H., X-ray study of synthetic Mg-Al serpentines and chlorites, *Am. Mineralogist, 44,* 143–152, 1959.

Greenwood, H. J., The system $NaAlSi_2O_6$-H_2O-argon: Total pressure and water in metamorphism, *J. Geophys. Res., 66,* 3923–3946, 1961.

Griggs, D. T., Deformation of rocks under high confining pressure, *J. Geol., 44,* 541–577, 1936.

Griggs, D. T., and J. D. Blacic, The strength of quartz in the ductile regime (abstract), *Trans. Am. Geophys. Union, 45,* 102, 1964.

Griggs, D. T., and J. D. Blacic, Quartz: anomalous weakness of synthetic crystals, *Science, 147,* 292–295, 1965.

Griggs, D. T., and John Handin, Observations on fracture and a hypothesis of earthquakes, *Geol. Soc. Am. Mem., 79,* 347–363, 1960.

Griggs, D. T., F. J. Turner, and H. C. Heard, Deformation of rocks at 500° to 800°C., *Geol. Soc. Am. Mem., 79,* 39–104, 1960.

Haasen, Peter, and A. W. Lawson, Jr., Der Einfluss hydrostatischen Druckes auf die Zugverformung von Einkristallen, *Z. Metallk., 49,* 280–291, 1958.

Handin, John, An application of high pressure in geophysics, *Trans. Am. Soc. Mech. Engrs., 75,* 315–324, 1953.

Handin, John, Strength at high confining pressure and temperature of serpentinite from Mayaguez, Puerto Rico, in *A Study of Serpentinite, Natl. Acad. Sci.—Natl. Res. Council Publ., 1188,* 126–131, 1964.

Handin, John, and R. V. Hager, Jr., Experimental deformation of rocks under confining pressure: Tests at room temperature on dry samples, *Bull. Am. Assoc. Petrol. Geologists, 41,* 1–50, 1957.

Handin, John, and R. V. Hager, Jr., Experimental deformation of rocks under confining pressure: Tests at high temperature, *Bull. Am. Assoc. Petrol. Geologists, 42,* 2892–2934, 1958.

Handin, John, R. V. Hager, Jr., M. Friedman, and J. N. Feather, Experimental deformation of sedimentary rocks under confining pressure: Pore pressure tests, *Bull. Am. Assoc. Petrol. Geologists, 47,* 717–755, 1963.

Handin, John, and D. W. Stearns, Sliding friction of rock (abstract), *Trans. Am. Geophys. Union, 45,* 103, 1964.

Heard, H. C., and W. W. Rubey, Possible tectonic significance of transformation of gypsum to anhydrite plus water (abstract), *Geol. Soc. Am. Spec. Paper 76,* 77–78, 1963.

Hess, H. H., Serpentines, orogeny and epeirogeny, *Geol. Soc. Am. Spec. Paper 62,* 391–408, 1955.

Hess, H. H., and G. Otalora, Mineralogical and chemical composition of the Mayaguez serpentinite cores, in *A Study of Serpentinite, Natl. Acad. Sci.—Natl. Res. Council Publ. 1188,* 152–168, 1964.

Holser, W. T., and G. C. Kennedy, Properties of water, 5, Pressure-volume-temperature relations of water in the range 400–1000°C and 100–1400 bars, *Am. J. Sci., 257,* 71–77, 1959.

Hotz, P. E., and E. D. Jackson, X-ray determinative curve for olivines of compositions Fo_{80-95} from stratiform and alpine-type peridotites, *U. S. Geol. Surv. Prof. Paper 450-E,* E101–E102, 1963.

Hubbert, M. K., and W. W. Rubey, Role of fluid pressure in mechanics of overthrust faulting, 1, *Bull. Geol. Soc. Am., 70,* 115–166, 1959.

Jaeger, J. C., The frictional properties of joints in rock, *Geofis. Pura Appl., 43,* 148–158, 1959.

Jaeger, J. C., *Elasticity, Fracture and Flow,* 208 pp., Methuen Ltd., London, 1962.

Lapham, D. M., and H. L. McKague, Structural patterns associated with the serpentinites of southeastern Pennsylvania, *Bull. Geol. Soc. Am., 75,* 639–660, 1964.

Orowan, E., Non-Newtonian viscosity, continental drift and mountain building, Discussion on continental drift, *Proc. Roy. Soc. London,* 1964.

Paterson, M. S., Triaxial testing of materials at pressures up to 10,000 kg/cm^2, *J. Inst. Engrs., Australia, 36,* 23–29, 1964.

Paterson, M. S., and L. E. Weiss, Experimental deformation and folding in phyllite, submitted for publication, 1965.

Pistorius, C. W. F. T., Some phase relations in the system MgO-SiO_2-H_2O to high pressures and temperatures, *Neues Jahrb. Mineral., 11,* 283–293, 1963.

Rubey, W. W., and M. K. Hubbert, Role of fluid pressure in mechanics of overthrust faulting, 2, *Bull. Geol. Soc. Am., 70,* 167–206, 1959.

Terzhagi, K., Simple tests to determine hydrostatic uplift, *Eng. News-Record, 116,* 501–523, 1936.

Turner, F. J., D. T. Griggs, and H. C. Heard, Experimental deformation of calcite crystals, *Bull. Geol. Soc. Am., 65,* 883–934, 1954.

Whittaker, E. J. W., and J. Zussmann, Characterization of serpentine minerals by X-ray diffraction, *Mineral. Mag., 31,* 107–126, 1956.

Wilkinson, J. G. F., Some aspects of the alpine-type serpentinites of Queensland, *Geol. Mag., 90,* 305–321, 1953.

(Manuscript received May 7, 1965.)